



Efficient approach to produce functional polypropylene via solvent assisted solid-phase free radical grafting of multi-monomers

Dengfei Wang^{1,2} · Jian Wang¹ · Shuyan He² · Yibin Yan² · Jianwei Zhang¹ · Jie Dong¹

Received: 24 June 2020 / Accepted: 7 December 2021 / Published online: 3 January 2021
© The Author(s) 2021

Abstract

Herein an efficient approach to produce functional polypropylene via solvent assisted solid-phase grafting process is reported, in which acrylic acid, methyl methacrylate and maleic anhydride are used as multi-monomers, 2,2'-azobis(2-methylpropionitrile) as initiator and ether as swelling solvent and carrier. The effects of various factors such as the swelling solvent species and dosage, swelling time and temperature, monomer and initiator concentrations, reaction time and temperature, nitrogen flow rate and the stirring speed on the grafting percentage and grafting efficiency were investigated. To verify the polar species was grafted onto polypropylene, the resulted polymers were characterized by Fourier transform infrared spectroscopy, scanning electron microscopy, X-ray diffraction analysis, water contact angle measurement, tensile strength and melt flow rate measurement. All the results showed that using the ether assisted solid-phase free radical grafting process is an efficient and versatile approach to produce functional polypropylene.

Keywords Functional polypropylene · Ether · Multi-monomers · Soaking · Grafting

Introduction

Polypropylene (PP) is one of the most widely used polymers in industry, as fiber, film and pipe, because it has many advantageous properties such as easy processing, high chemical resistance, flexibility, low density, adequate mechanical properties and low cost. Due to the low surface energy and lack of reactive functional groups on its molecular chains, PP is not compatible with a wide range of other polymers and fillers and also has printing and adhesion problems [1–4]. The methods that have been used for obtaining functional modification of PP include chlorination [5], hydroperoxidation [6], hydrogen abstraction from tertiary carbons, followed by ozonolysis [7], in situ copolymerization and grafting copolymerization [8]. Among these methods, the

grafting copolymerization of polar vinyl monomers onto PP offers a very feasible approach [9].

The conventional processes of grafting functional groups onto PP backbones can be performed in solution, melt, aqueous suspension, or the solid-state, all of which suffer from several drawbacks. In the solution grafting process all of the initiator, monomers and PP are dissolved into a solvent to form a homogeneous reaction media. After the functional groups are grafted onto the PP backbones, it is difficult to remove the solvent from the final product and usually additional waste streams are created [10–12]. Melt processing operating in extruders, is a proven technique for grafting modification of PP and has been applied on a large scale. Generally, extruders have numerous advantages that make them ideal for polyolefin modification and some polymerization processes. These include good mixing, reasonable heat transfer and good pumping abilities for high viscosity materials. One of the major disadvantages of reactive extrusion is this process must be performed in the molten phase, therefore resulting in serious coupling, crosslinking and degradation [13, 14]. In the aqueous suspension process, monomers and initiators are dissolved into the water before adding to the polypropylene matrix, and then grafting reactions are initiated in suspension state. However, due to the hydrophobic characteristic of PP, the type and amount

✉ Jian Wang
mrwj163@163.com

¹ Provincial Key Laboratory of Oil and Gas Chemical Technology, College of Chemistry and Chemical Engineering, Northeast Petroleum University, Daqing City 163318, China

² Daqing Petrochemical Research Center, Petrochemical Research Institute of PetroChina, Daqing City 163714, Heilongjiang Province, China

of monomers are limited due to the solubility in water. At the same time, the mass transfer efficiency of monomer on polypropylene particles is also limited, resulting in low grafting efficiency [15–17]. Compared with the other grafting methods, the solid-phase grafting process boasts many advantages such as lower reaction temperature, freedom from the need for solvent recovery and simpler equipment requirement [18, 19]. However, the main disadvantage of this process is that most monomers are grafted only on the surface of the PP particles, and the interior and any pores of the PP remain nonpolar [20]. To resolve the poor uniformity of the grafted products, the supercritical carbon dioxide (SC CO₂) assisted solid-phase grafting process was introduced as a high-efficiency and environmentally-friendly method in recent years [21–26].

As a known swelling agent for most polymers, SC CO₂ can dissolve many small molecules [24]. This unique property provides an opportunity to use SC CO₂ as a solvent and swelling agent to impregnate polar vinyl monomers and initiators uniformly into PP. The degree of swelling in the PP as well as the partitioning of small molecules penetrant between the swollen polymer phase and the fluid phase can be easily controlled by its supercritical phase parameters. Grafting copolymerization is then initiated thermally within the swollen PP to form a grafted branch-chain, either in the presence of SC CO₂ or after venting the CO₂ replacement with N₂. These procedures are so-called SC CO₂ assist solid phase grafting process. It was found that SC CO₂ assist solid phase grafting process significantly increased the homogeneous distribution of grafting branch-chain onto the surfaces and micropores of PP particles and remained its versatile physical properties though introducing the grafting branch chain. Unfortunately, CO₂ is gas at ambient condition, its supercritical states (T_c = 31.1 °C, P_c = 7.38 MPa) are attained by compression and heat [25–27]. It has strict requirements on the pressure rating of the experimental device. The amount of samples obtained in each experiment was also relatively small [24, 28]. So the large-scale application of this process for functionalization PP hasn't been reported so far.

Interestingly, ether also can dissolve small organic molecules and swell most polymers like SC CO₂. Besides, its boiling point is 36 °C, which is liquid at room temperature. So it could swell polymers under normal pressure, which will decrease cost and improve the security of experimental device. Moreover, it is easy for ether to transform between liquid and gas. So it is easy to remove and recycle ether from PP swell reaction system. This fact prevents products and the environment from being polluted.

In this study, ether was used to replace SC CO₂ as swelling solvent and carrier in solvent assisted solid-phase free radical grafting copolymerization of multi-monomer AA/MMA/MAH onto PP. Crystallinity, morphology,

hydrophilicity and mechanical property of the grafted products were studied, and very satisfactory results were obtained. As far as we know, little attention has been paid to the ether solvent assisted solid-phase free radical grafting process in preparing a functional copolymer. Therefore it is of significances for academic and industrial researchers.

Experimental section

Materials

PP (T30S) without any additive was kindly provided by Daqing Petrochemical Company. Acrylic acid (AA) and methyl methacrylate (MMA) were produced by the Tianjin Special Chemical Reagent Development Center (AR grade) and used after purification by vacuum distillation. 2,2'-Azobis(2-methylpropionitrile) (AIBN) was purchased from the Shenyang Donghua Chemical Company (AR grade) and was used after recrystallization twice from methanol. Pure AA, MMA and AIBN were stored in icebox before use. Maleic anhydride (MAH), methanol, ether, acetone, analytical grade; nitrogen with a purity of 99.9% were supplied by Daqing petrochemical Company and used as received.

Grafting procedures

The solvent assisted solid-phase free radical grafting process was composed of two steps as was done in SC CO₂ assist solid phase grafting process [20, 21, 26, 29]: the soaking step and the grafting copolymerization reaction step. During the soaking step, the monomer and initiator were diffused into the ether-swollen PP particles. First, a three-necked flask equipped with a twin-blade mechanical stirrer, a nitrogen inlet, and a thermometer was flushed with nitrogen for 3–5 min at room temperature. The temperature of the flask was maintained with an accuracy of ± 1.0 °C. Multi-monomers AA, MMA, MAH and initiator AIBN were dissolved into ether beforehand. 10 g PP particles and a suitable amount of ether solution were placed into the reactor. Then the solution was agitated to swell PP in an oil bath at the given temperature to ensure that this mixture was absorbed by PP granules. Subsequently ether was released by heating after the required soaking time had elapsed. After venting ether, the grafting copolymerization reaction step was operated immediately. The impregnated grains were heated up to a given reaction temperature, and kept at this temperature for the desired reaction time under nitrogen. Before characterization, PP-g-AA–MMA–MAH samples were purified by Soxhlet extraction in acetone for 12 h to remove unreacted monomers and initiator, and then dried in vacuum at 50 °C for 24 h. After drying, the extracted samples were weighed

and re-extracted until the weight of the samples was constant. The possible structure and reaction mechanism of AA, MMA and MAH grafting onto PP are discussed in Refs. [2, 30, 31] and described in Fig. 1. During the grafting process, degradation and rearrangement of PP radicals may occur, as well as homopolymerization of monomers, so it is necessary to remove self-polymerized by-products from PP-g-AA-MMA-MAH by solvent extraction [32].

Calculation of grafting percentage (Gp) and grafting efficiency (Ge)

Gp and Ge were calculated according to Eqs. (1) and (2).

$$Gp = \frac{m_2 - m_1}{m_1} \times 100\% \tag{1}$$

$$Ge = \frac{m_2 - m_1}{m_0} \times 100\% \tag{2}$$

where m_0 is original mass of PP in sample, m_1 is sample mass after extraction, and m_2 is total mass of feeding monomers.

Characterization

Fourier transform infrared (FTIR) spectral analysis, scanning electron microscope (SEM) analysis, water contact angle measurement, Gel permeation chromatography (GPC) analysis, thermogravimetric (TGA) analysis, X-ray diffraction (XRD) analysis, MFR and mechanical properties measurements were done according to the literature [6, 20]. The FTIR spectra were recorded on a Perkin-Elmer 1760-X infrared spectrometer from 4000 to 400 cm^{-1} with a 0.5 cm^{-1} resolution. The fracture surfaces of the samples were studied with a JEOL JSM-6360LA scanning electron microscope operated at 15 kV. Surfaces of the samples were coated with chromium (3 nm) before the measurement with a JEOL JFC-1600 Auto Fine Coater. Contact angles of the nascent PP and grafted samples were determined using a Shanghai Zhongchen Co. Ltd. JC2000C1 contact angle goniometer at ambient temperature. The average MWs, including the number-average molecular weight (M_n), weight-average molecular weight (M_w), and viscosity-average molecular weight (M_v), were measured at 135 °C by a Waters 150CV GPC instrument (Waters Co., Milford, Massachusetts) with *o*-dichlorobenzene as the solvent. Thermogravimetric analysis (TGA) of grafted copolymers was carried out on a Diamond TG/DTA thermal analyzer at a heating rate of

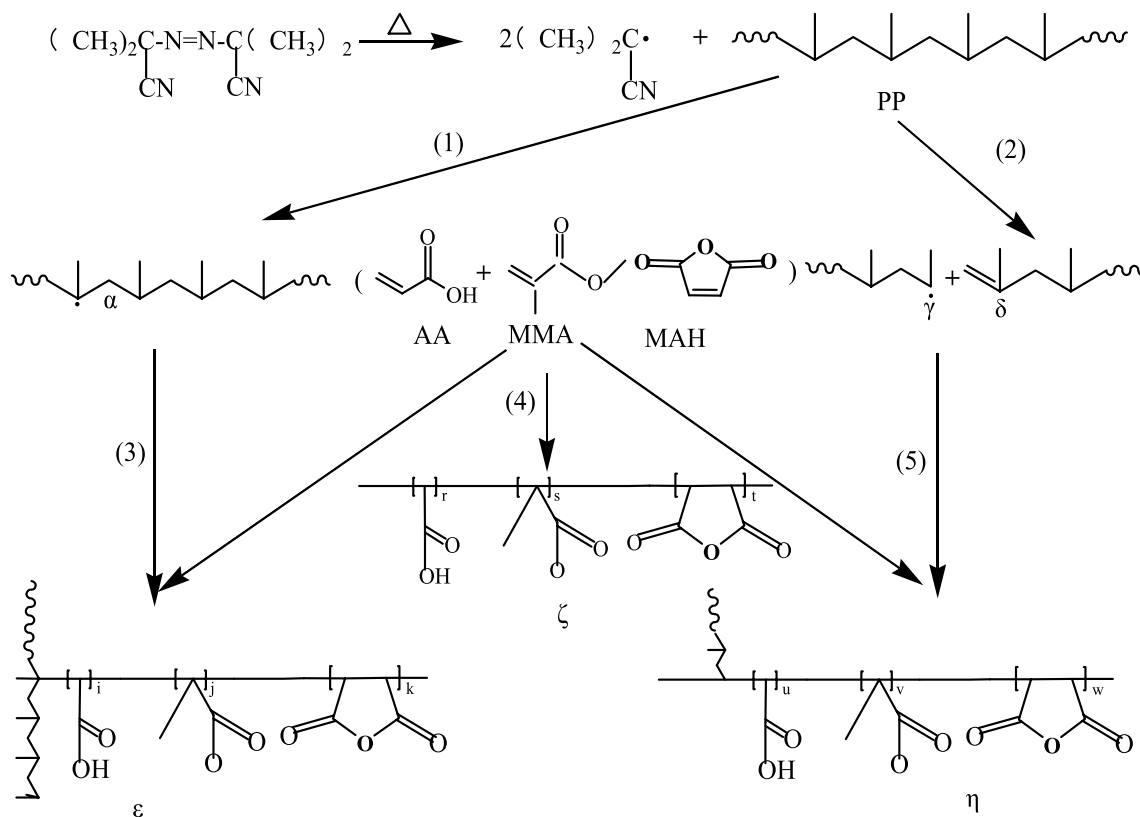


Fig. 1 Schematic illustration of possible grafted PP structure and reaction mechanism

10 °C/min from room temperature to 500 °C. The crystallization behavior of the grafted samples was determined by X-ray diffraction (XRD) analysis with a D/MAX-2200 X-ray diffractometer (Rigaku Co., Tokyo, Japan) with Cu target radiation over the range $2\theta = 10^\circ\text{--}80^\circ$. The tube voltage was 40 kV, and the tube current was 30 mA. The samples were processed in 0.4 mm thick films by compression molding at 200 °C for 1 min. MFR was measured with a Takara X-416 Melt Indexer, (Takara Thermistor Instruments, Japan) Measurement was performed at 230 °C with a load of 2.16 kg. Tensile properties of samples were investigated on a universal tensile tester (Instron 1122) using a load of 20.0 kg. An average of five test results was calculated and reported.

Results and discussion

Grafting parameters

Effect of swelling solvent species

In this work, the soaking experiments were conducted under conditions at which swelling solvent, AA, MMA, MAH and AIBN exist as a single phase. To determine the optimal operation conditions, the effects of the swelling solvent species and dosage, swelling time and temperature, monomer and initiator concentrations, reaction time and temperature, nitrogen flow rate and stirring speed on Gp and Ge were studied, and the results were shown in Table 1 and Figs. 2, 3, 4, 5, 6, 7, 8, 9 and 10.

According to the literature [33, 34], some organic solvents can be used as swelling solvent of PP and carrier of multi-monomers. Table 1 summarizes the Gp and Ge data obtained in the presence of varying swelling solvent species. The soaking experiments were carried out at 29 °C for 10 h, followed by thermal reaction at 80 °C for 1.5 h with AIBN as initiator. The solvent dosage was 1.4 ml/gPP. The mass ratio of PP/AIBN/monomers was 100:0.5:6. The nitrogen flow was 30 ml s⁻¹. The stirring speed was 50 r min⁻¹.

As can be seen from Table 1, the Gp and Ge of ether were highest, followed by hexane while the others were not ideal for using as a swelling solvent. There is a great

Table 1 Effect of swelling solvent species on grafting reaction

Swelling solvent species	Gp, %	Ge, %
Ethanol	1.13	17.8
Acetone	1.64	27.3
Petroleum ether (30–60 °C)	1.60	26.7
Ether	3.29	54.8
Hexane	2.81	46.7
Heptane	2.40	40.0

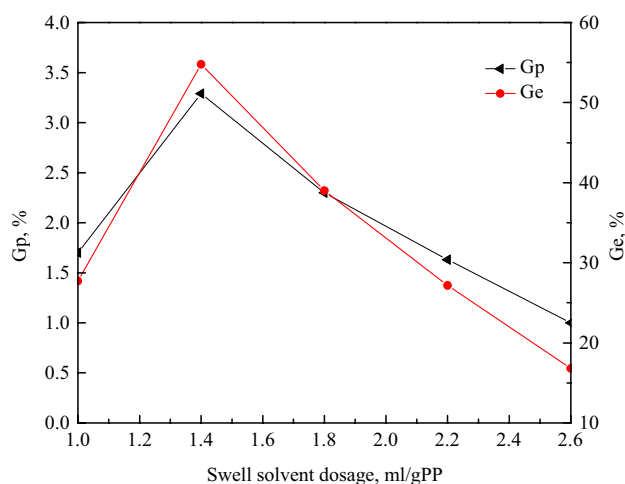


Fig. 2 Influence of swelling solvent dosage on Gp and Ge (other conditions were same as those in Table 1)

difference between solubility and diffusion coefficient of ethanol, acetone, petroleum ether in PP and ether/hexane. As a rule of “likes dissolve each other”, substances incline to dissolve in the solvent which has a similar formation due to dominant intermolecular attraction [35]. The polarity of ethanol, acetone, petroleum ether is higher with compared to ether and hexane, which is similar to PP. So the former solvent could not swell PP particles well. Little of monomers and the initiator were adsorbed on the particle surface, and most of them remained in the swelling solvent, resulting in a low Gp and Ge. As to ether and hexane, they could swell PP efficiently. So monomers and the initiator easily diffused into particles with the assistance of solvent, which caused a high Gp and Ge. Considering Gp, Ge, environment and energy issues, ether was selected as a swelling solvent.

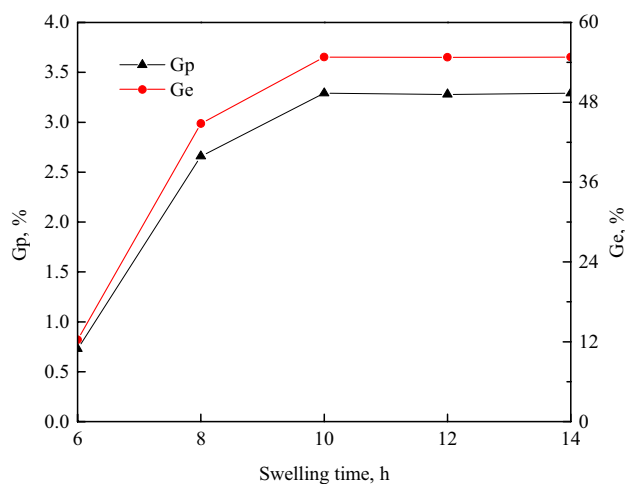


Fig. 3 Influence of swelling time on Gp and Ge (other conditions were same as those in Table 1)

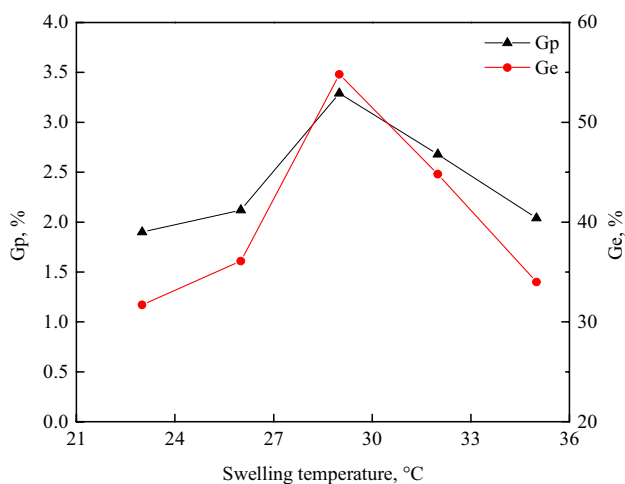


Fig. 4 Influence of swelling temperature on Gp and Ge (other conditions were same as those in Table 1)

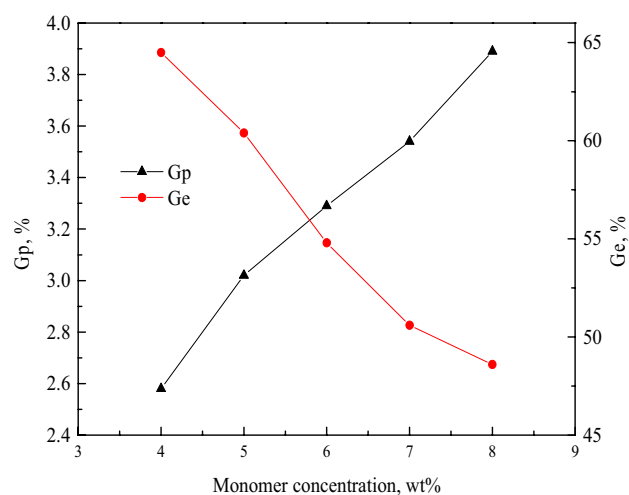


Fig. 6 Influence of monomer concentration on Gp and Ge (other conditions were same as those in Table 1)

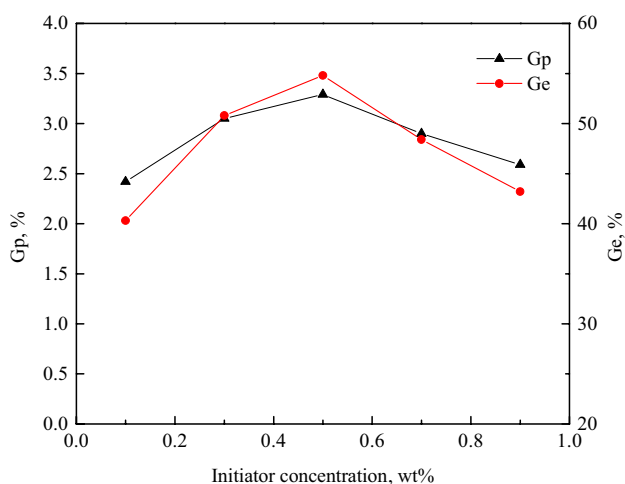


Fig. 5 Influence of initiator concentration on Gp and Ge (other conditions were same as those in Table 1)

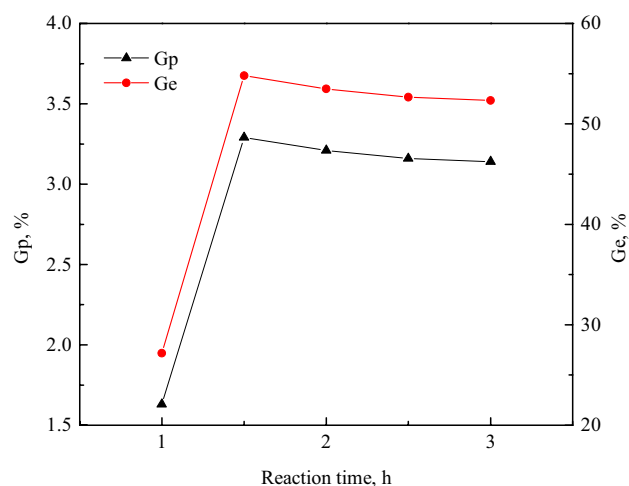


Fig. 7 Influence of reaction time on Gp and Ge (other conditions were same as those in Table 1)

Effect of swelling solvent dosage

Figure 2 shows swelling solvent dosage influence on Gp and Ge with ether as a swelling solvent and carrier. The other conditions are the same as those in Table 1. As can be seen from the curve, Gp and Ge at first increase with swelling solvent dosage, then decrease after the swelling solvent dosage reaching 1.4 ml/gPP. This phenomenon can be explained as follows: According to D. A. Blackadder's study [36, 37], the soaking temperature is well below PP's melting point, semicrystalline parts do not dissolve wholly in organic solvents. However, even at low temperatures, most solvents can penetrate the amorphous regions to some degree, resulting in the solvation of individual segments of PP chains and overall swelling of the specimen. In this work, the amount of AIBN/

monomers was fixed. An increase in the swelling solvent dosage led to the increase of solubility in ether, which was not favorable for the impregnation of AIBN/monomers in PP matrix because AIBN/monomers distributes between solvent phase and PP matrix; on the other hand, the increase of swelling solvent dosage resulted in an increase in the swell or plasticizing content of the PP matrix, which made the diffusion of monomer and initiator in PP easier, and this was favorable for grafting reaction. In the low swelling solvent dosage range, the first factor was always predominant. At high swelling solvent dosage the stronger solubility of ether made the absorption of monomers and the initiator into the PP matrix more difficult. The maximum of Gp and Ge at swelling solvent dosage of 1.4 ml/gPP indicated a balance of the two opposite factors. The results are similar to

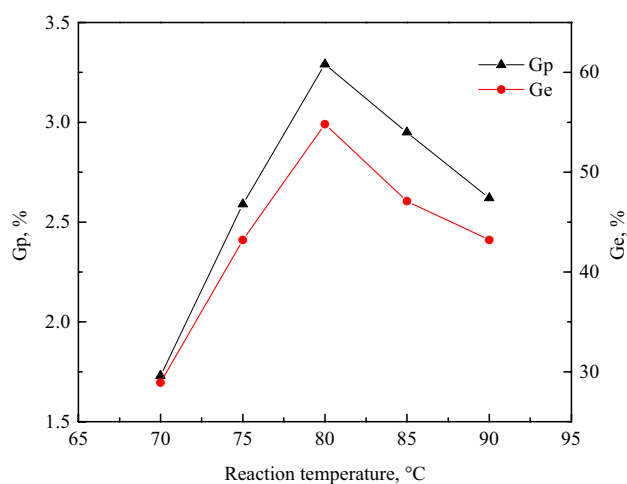


Fig. 8 Influence of reaction temperature on Gp and Ge (other conditions were same as those in Table 1)

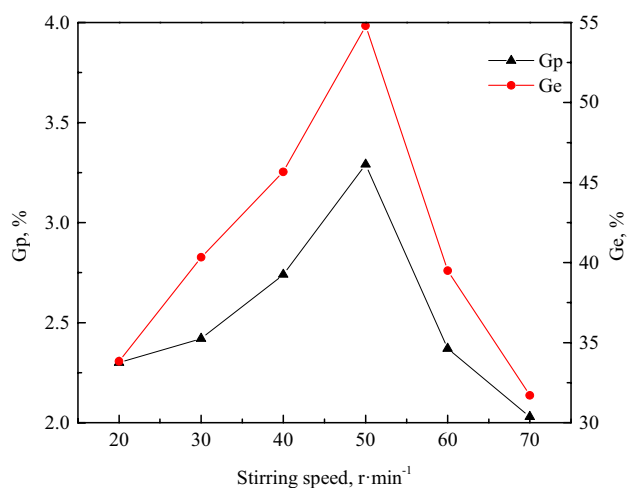


Fig. 10 Influence of stirring speed on Gp and Ge (other conditions were same as those in Table 1)

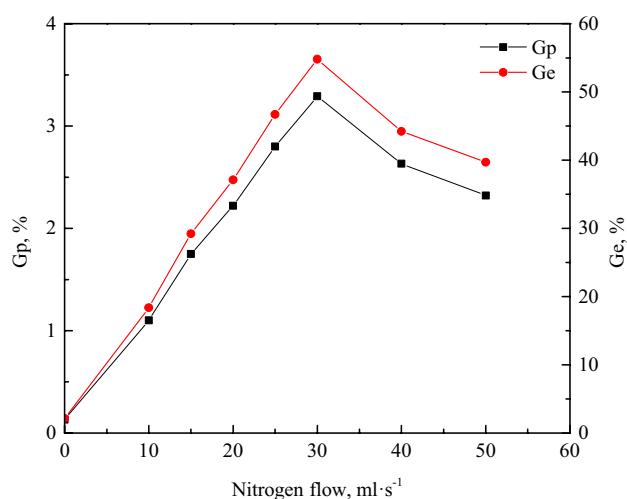


Fig. 9 Influence of nitrogen flow rate on Gp and Ge (other conditions were same as those in Table 1)

increasing swell pressure in SC CO₂ assist the solid phase grafting process [38, 39].

Effect of swelling time

Figure 3 shows the effects of swelling time on on Gp and Ge with ether as a swelling solvent and carrier. The other conditions are the same as those in Table 1. After an initial quick increase of Gp and Ge, the curves became parallel as swelling time extending to 10 h. As was expected, a prolonged swelling time was benefit for PP swell and diffusion of monomers/initiator into PP matrix, so Gp and Ge were increased rapidly. But when the swelling time was over 10 h, diffusion of monomers and initiator reached a dynamic balance between solvent and solid particles. In other words,

soaking equilibrium can be reached within 10 h. In fact, the soaking process was a distribution procedure that allots the monomer and initiator heterogeneously between solution-phase and PP matrix [40]. The monomer and initiator were first dissolved into the ether, then diffused and absorbed onto the grafting areas of PP with the aid of ether. As the soaking time increased, the diffusion of monomer and initiator molecules onto the PP particles surfaces also increased, so the grafting percentage was growing. The parallel of grafting percentage may be attributed to the saturation of active sites on PP backbone by diffusion and absorbance of monomer and initiator, which formed a diffusion barrier on the grafting zones. This also implied that the swell ability of ether towards this PP matrix had a limited value. The results were in agreement with the findings obtained by using SC CO₂ as a swelling solvent and carrier [26].

Effect of swelling temperature

Swelling temperature is one of the important factors that control the soaking process [35]. Figure 4 shows the relationship between swelling temperature and Gp, Ge with ether as a swelling solvent and carrier. The other conditions are the same as those in Table 1. It can be seen that Gp and Ge increase with increasing in swelling temperature and reach a maximum at 29 °C and then decrease fast. This is due to thermal motion of small molecules like monomers, AIBN and PP chains accelerate with increasing swelling temperature, which is benefit for swell of PP particles and diffusion of monomers and initiator [41]. However, the boiling point of ether is 36 °C. When swelling temperature rose to 29 °C, ether vaporizes in intensity and forms a huge cloud of gas. A crust of monomers and initiator is left on the surface of the PP. When vent ether

after swell process, most of monomers will be carried away. Besides, monomers left on the PP surface incline to homopolymerization, which is separate as by-products in Soxhlet extraction. So Gp and Ge began decreasing.

Effect of initiator concentration

During the graft polymerization, the initiator, AIBN, generates two free radicals upon heating to its decomposition temperature. The radicals abstracted hydrogen atoms from the backbone of PP polymer, leading to the formation of the macromolecular radicals of PP [42]. The macromolecular radicals could initialize the grafting polymerization of the functional monomer onto the backbones to form desired modified polymers or could undergo polymer chain scission to produce lower molecular weight polymers, as shown in Fig. 1. The effects of the initiator concentrations on Gp and Ge were shown in Fig. 5. Gp and Ge reach their peak when AIBN concentration is 0.5 wt% with ether as a swelling solvent and carrier. The other conditions are the same as those in Table 1. It can be seen that as AIBN amount increases, Gp and Ge initially increase and pass through a maximum. The initial increase in Gp and Ge is caused by the increased amount of free radicals for the chain transfer to the polymer backbone. However, Gp and Ge tend to decrease if the initiator concentrations rise continually. This is because that the concentration of the initiator is so high that the free radicals have more chance to meet with each other. Radical activity is too high to exist in isolation, so termination reaction occurs easily. For this reason, side reaction (e.g. bi-radical termination, β chain scission, chain transfer) increases, which leads to the decrease of Gp and Ge.

Effect of monomer concentration

Figure 6 shows the effect of monomers concentration on Gp and Ge with ether as a swelling solvent and carrier. The other conditions are the same as those in Table 1. It can be seen that Gp increases constantly with the concentration of the monomers but Ge decreases straightly. As the concentration of monomers goes high, more monomers will be impregnated into the PP matrix. As we all know, a swelling agent mainly swells the amorphous regions of PP matrix. Because of the existence of crystalline domains in PP matrix, it can only swell the polymer to some extent. When the swell degree is fixed, the absorbance balance of monomer in solvent phase and PP matrix is obtained. An increase of monomer concentration cannot increase the grafting percentage. The extra amount of monomer will auto polymerization. So Ge is constantly decreased..

Effect of reaction time

Figure 7 shows the effect of reaction time on Gp and Ge with ether as a swelling solvent and carrier. The other conditions are the same as those in Table 1. Gp and Ge increased initially with prolongation of reaction time and then tended to decline slightly. This is because all the AIBN had been consumed and/or all the monomers had been polymerized after a certain reaction time. The grafting polymerization had been nearly over. However, the degradation reaction of PP macromolecular chains became serious if prolonged reaction time. So Gp and Ge tended to decline slightly.

Effect of reaction temperature

Figure 8 shows the effect of reaction temperature on Gp and Ge by varying reaction temperature from 70 to 90 °C with ether as a swelling solvent and carrier. The other conditions are the same as those in Table 1. From the Fig. 7, it was observed the peak of curves was obtained at 80 °C. Reaction temperature effect on Gp and Ge is closely related to initiator's decomposition half-life. The decomposition half-lives of AIBN are 5 h, 2.5 h, 1.3 h, 0.68 h, 0.36 h at 70 °C, 75 °C, 80 °C, 85 °C, 90 °C respectively [43]. At a low reaction temperature, the decomposition of AIBN was incomplete. Most of monomers were thermal initiation to homopolymerization. When reaction temperature ranges from 70 to 80 °C, more free radicals are present, so monomers tend to graft alternatively onto the PP backbone, causing Gp and Ge to increase rapidly. At 80 °C, the decomposition rate of AIBN was compatible with the grafting polymerization rate, so Gp and Ge reached at peak. However, if the reaction temperature increased continually, the decomposition rate of the initiator would exceed the grafting polymerization rate, resulting in the surplus of free radicals in the sites of grafting reaction. So side reactions such as homo-polymerization of monomers and termination of free radicals occurred badly. These side reactions consumed a lot of initiator and monomers, resulting in Gp and Ge decrease.

Effect of nitrogen flow rate

Figure 9 shows the optimal nitrogen flow rate is 30 ml/min with ether as a swelling solvent and carrier. The other conditions are the same as those in Table 1. The reaction of oxygen with free radicals formed inactive peroxy radicals, such as: $M_x \cdot + O_2 \rightarrow M_x-O-O \cdot$ [29]. Termination reaction occurred between two peroxy radicals or peroxy radicals and other radicals [44]. These reactions decreased the initiation efficiency of AIBN, leading to a low Gp and Ge. As a protective gas, nitrogen drove oxygen out from the reactor, resulting in the increase of Gp and Ge with nitrogen flow increase. However, the whole reaction system was not

completely sealed and the monomers were inclined to volatile. So nitrogen would take away some monomers. Increase of nitrogen flow, this effect became more and more serious. When the nitrogen flow increased to 30 ml/min or even more, this effect exceeded the protective effect. So Gp and Ge went down with nitrogen flow increase.

Effect of stirring speed

Figure 10 shows the relationship between stirring speed and Gp, Ge with ether as a swelling solvent and carrier. The other conditions are the same as those in Table 1. It can be seen that the temperature dependences of Gp and Ge have similar trends, which exhibit maximum at 50 r/min. As well known, stirring is good for mass and heat transfer. However, with the assistant of solvent swell process, stirring having little or no impact on monomers/initiator transferring to PP matrix. So the main effect of the stirring was on heat transfer in this work. When the stirring speed was set at 20 r/min, stirring was too low to transport excessive polymerization heat away from warm region of the reactor. Most of the monomers in the hotspot were thermally initiated to homo-polymerization rather than grafting on PP. Increasing the stirring speed from 20 to 50 r/min, polymerization heat began to be removed effectively. Hence Gp and Ge went significantly up with stirring speed increase. When the stirring speed is raised over 50 r/min, PP granules were stirred to the reactor wall. Due to polymerization heat, PP would stick to the reactor wall, homo-polymerization of the monomers would be accelerated and disadvantageous to the graft

polymerization. Therefore, a stirring speed of 50 r/min is appropriate for practical applications.

Characterization

FTIR spectra

The grafting of AA, MMA and MAH onto PP was confirmed by FTIR spectroscopy, as illustrated in Fig. 11. Compared with the spectrum of nascent PP, four new characteristic absorption bands are observed in the grafted PP. They appear at 1858 cm^{-1} (asymmetrical C=O stretching of anhydride), 1781 cm^{-1} (symmetric C=O stretching of anhydride), 1735 cm^{-1} (symmetric C=O stretching of ester) and 1710 cm^{-1} (C=O stretching of carboxylic acid). Infrared spectroscopy is the most commonly used method in determining MAH content in the polymer. In Ref. [45], two new absorption peaks were observed at 1860 and 1780 cm^{-1} , corresponding to the symmetric and asymmetric stretching of the two C=O groups in the resulting succinic anhydride group of PP-g-MAH. The 1732 cm^{-1} that is attributable to the ester carbonyl stretching vibration of PP-g-PMMA was confirmed by Zhao [46]. The methyl methacrylate (MMA) and acrylic acid (AA) bi-monomers grafting on PP using corona discharge surface modification method was studied by K. S. Abudonia, and 1749 cm^{-1} (symmetric C=O stretching of ester) and 1712 cm^{-1} (C=O stretching of carboxylic acid) were confirmed [47]. These facts all suggest that AA, MMA and MAH had been grafted onto PP successfully in this work.

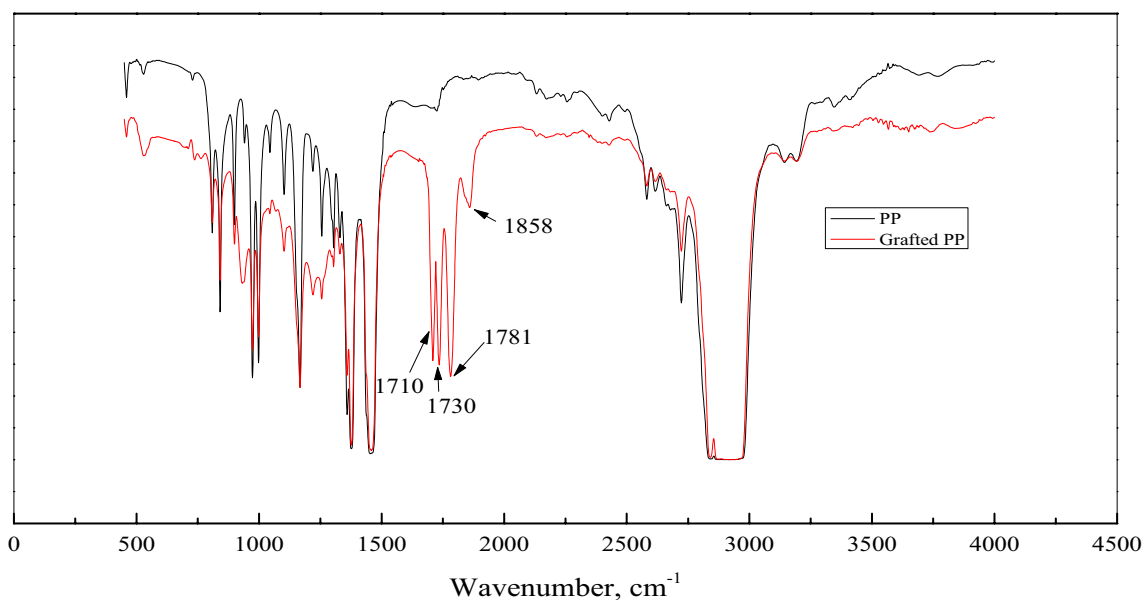


Fig. 11 FTIR spectra of nascent and grafted PP

SEM

Figure 12 displays SEM micrographs of nascent and grafted PP. Compared with nascent PP (Fig. 11a, b), the morphologies of grafted PP (Fig. 11c, d) were significantly different. The inner and outer surfaces of grafted PP were rougher than the original PP. This indicated that grafting reaction occurred in the inner and outer of PP particles simultaneously.

XRD spectra

In order to investigate the crystallization behavior of the grafted samples, a WAXD study is performed. Figure 13 shows the XRD spectrum of the nascent PP and grafted PP. As is shown, the characteristic diffraction peaks of α -PP at $2\theta = 14.1^\circ$, 16.8° , 18.5° , 21.2° , 21.8° , and 25.5° , corresponding to specific crystallographic planes (110), (040), (130), (131), (111), and (041), are all present in PP and grafted PP. However, obvious diffraction peaks at $2\theta = 15.9^\circ$ corresponding to β hexagonal system of PP, indicating that β crystal forms is present in grafted PP [48]. Moreover, compared with nascent PP, the diffraction peak's intensity of grafted PP becomes weaker, which indicates the grafted branch-chains may lead to the slight destruction of tacticity [41].

Fig. 12 SEM of nascent and grafted PP [Surface and of inner morphology of nascent PP (a, b); surface and of inner morphology of grafted PP (c, d)]

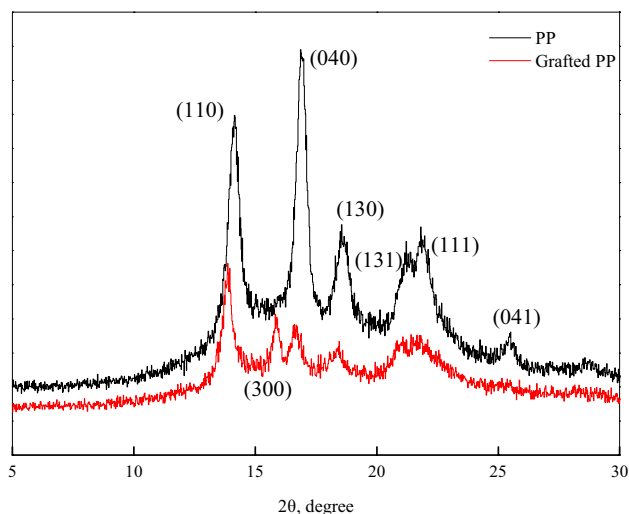
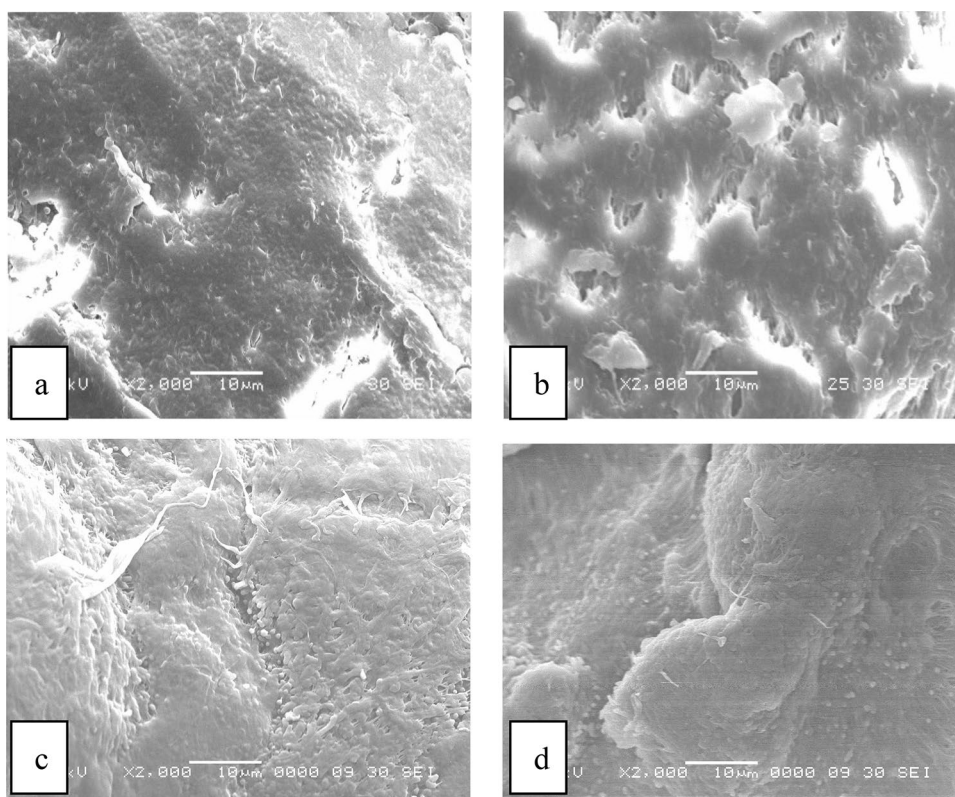


Fig. 13 XRD spectra of nascent and grafted PP

Contact angle

The water contact angle of nascent PP and grafted PP. Compared with nascent PP (91°), the water contact angle of modified PP significantly decreased to 79° , indicating this method could improve PP polarity and hydrophilic property effectively.

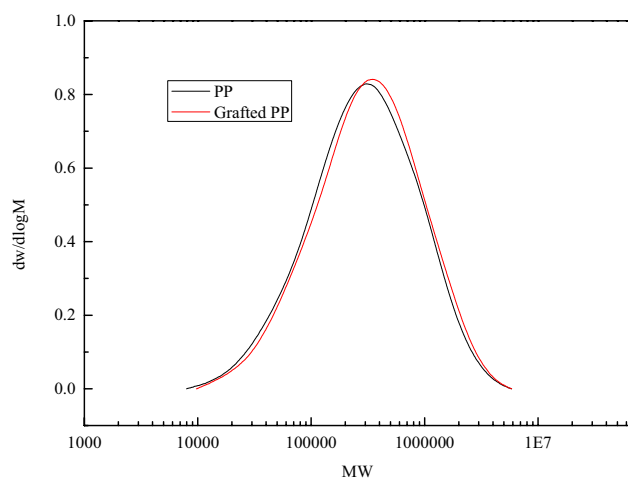


Fig. 14 GPC curves for nascent and grafted PP

Table 2 GPC results analysis of the samples

Samples	Mn	Mw	Mz	Mv	PDI
PP	105052	327529	746769	283733	3.11778
Grafted PP	154669	491320	1141643	424436	3.17659

Table 3 Tensile properties and MFR results of samples

	MFR, g/10 min	Tensile strength, MPa
PP	3.5	35.7
Grafted PP	3.8	35.4

MW determination

Figure 14 depicts the MWD curves of nascent and grafted PP. From the comparison of the two figures, one can find that both of them show very similar MWD, which indicates that the two polymers have a very closer PDI. To describe the difference between the two polymers, the MFR and detailed GPC testing results have been listed in Tables 2 and 3. As is seen, the MW values (Mn, Mz, Mv, and Mw) of the grafted polymer PP-g-AA-MMA-MAH was obviously larger than those of pure PP. This means that the grafting reaction occurs at the high and low molecular weight parts of polypropylene simultaneously. However, the monomers are more likely to be grafted onto low molecular weight parts of polypropylene, which is comparable with the MFR results. As is shown in Fig. 1, the potential side reaction during the grafting process is the undesired polymer chain scission and homopolymerization of the monomer, leading to low molecular weight and mechanical properties of the grafted

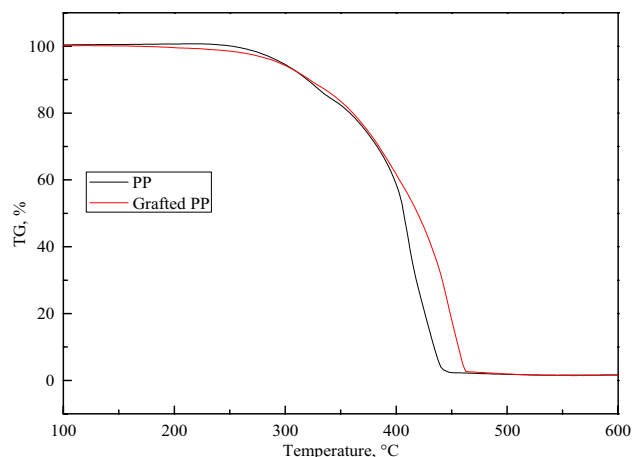


Fig. 15 TGA patterns of the nascent and grafted PP

polymers. The GPC results indicate that the solvent assisted solid-phase free radical grafting system had mild reaction conditions and that the grafting reaction mostly occurred on the shorter molecular chains of PP. Furthermore, the addition of AA-MMA-MAH largely suppressed the degradation of the main chains of PP, which is beneficial for making high-performance functional PP.

TGA

Figure 15 shows the TGA results of the nascent PP and grafted sample. It can be seen from this figure that grafted PP had a lower onset thermal degradation temperature. The temperature when the nascent PP lost 50% of its mass was 375.8 °C comparing 374.3 °C of the grafted PP, while the 100% degradation temperature of nascent PP was 20 °C below the grafted one. As we have discussed before, the addition of MAH, AA and MMA can promote the PP macroradicals to react with the monomers before the degradation of the main chains of PP. However, there are still some PP macroradicals that would degrade into small molecules. So the onset of thermal degradation temperature is lower than the nascent PP. In addition, the polarity monomers resulted in the redistribution of the density of the electron cloud of the intermolecular chemical bonds, which strengthened the bond energy between the atoms and enhanced the thermal stability of PP. So the 100% degradation temperature of nascent PP was lower than the grafted one.

Tensile properties and MFR

The tensile properties and MFR of grafted samples were determined and the results were listed in Table 3. The tensile strength and MFR of grafted PP (35.4 MPa and 3.8 g/10 min) is similar to raw material (35.7 MPa and 3.5 g/10 min), indicating that the grafting reaction didn't

change PP mechanical properties significantly. This result could be explained as grafting chains are so short that they hardly influence PP macromolecular chains. Due to most of their copolymerization sites lie in the micropores and defects of PP granules. These restricted spaces suppress the grafted branch-chains propagation. Moreover, the reaction conditions are too moderate to initiate degradation and the crosslinking reaction of PP macromolecular chains.

Conclusion

PP-g-(AA–MMA–MAH) grafted copolymer could be prepared by solvent assisted solid-phase free radical grafting of multi-monomer acrylic acid (AA), methyl methacrylate (MMA) and maleic anhydride (MAH) onto PP and ether as swelling solvent and carrier. The optimum grafting condition is obtained at swelling solvent of ether, swelling solvent dosage of 14 ml, swelling time of 10 h, swelling temperature of 26 °C, AIBN concentration of 0.5 wt%, monomer concentration of 6 wt%, the reaction time of 1.5 h, reaction temperature of 80 °C, nitrogen flow of 30 ml/s and stirring speed of 50 r/min with Gp of 3.29 wt% and Ge of 54.8%. As is seen, solvent assisted solid-phase free radical grafting process is an easy and efficient approach to produce functional polypropylene, which polar branch-chains can be controllable introduced with a dense and exact localization to the surface and inner of PP powder. Because the diffusion of monomers and the initiator had reached a dynamic balance between solvent and solid particles before the beginning of reaction, grafting reaction occurred in the inner and outer of PP particles simultaneously. Due to the introduction of short branch-chains in PP macromolecules, β crystal form was induced. Comparing with neat PP, the polarity and hydrophilic property of grafted samples was improved effectively; the bulk property, especially the tensile strength and MFR remains unchanged.

Open Access This article is licensed under a Creative Commons Attribution 4.0 International License, which permits use, sharing, adaptation, distribution and reproduction in any medium or format, as long as you give appropriate credit to the original author(s) and the source, provide a link to the Creative Commons licence, and indicate if changes were made. The images or other third party material in this article are included in the article's Creative Commons licence, unless indicated otherwise in a credit line to the material. If material is not included in the article's Creative Commons licence and your intended use is not permitted by statutory regulation or exceeds the permitted use, you will need to obtain permission directly from the copyright holder. To view a copy of this licence, visit <http://creativecommons.org/licenses/by/4.0/>.

References

- Chen Z, Huang D, Hwang J-Y (2019) Effect of styrene addition on chemically induced grafting of 4-vinylbenzyl chloride onto low-density polyethylene for anion exchange membrane preparation. *Polym Int* 68:972–978. <https://doi.org/10.1002/pi.5788>
- Han C, Zhang X, Chen D, Ma Y, Zhao C, Yang W (2020) Enhanced dielectric properties of sandwich-structured biaxially oriented polypropylene by grafting hyper-branched aromatic polyamide as surface layers. *J Appl Polym Sci* 137(34):48990. <https://doi.org/10.1002/app.48990>
- Munoz PAR, Bettini SHP (2016) Montmorillonite as support for peroxide in the melt grafting of maleic anhydride onto polypropylene. *J Appl Polym Sci* 133(42):44134. <https://doi.org/10.1002/app.44134>
- Asamoto H, Kimura Y, Ishiguro Y, Minamisawa H, Yamada K (2016) Use of polyethylene films photografted with 2-(dimethylamino)ethyl methacrylate as a potential adsorbent for removal of chromium (VI) from aqueous medium. *J Appl Polym Sci* 133(18):43360. <https://doi.org/10.1002/app.43360>
- Inagaki N, Tasaka S, Suzuki Y (1994) Surface chlorination of polypropylene film by CHCl_3 plasma. *J Appl Polym Sci* 51(13):2131–2137. <https://doi.org/10.1002/app.1994.070511304>
- Zhu B, Wang J, Dong Q, Song J (2010) Study on styrene and maleic anhydride grafted polypropylene in water suspension system. *China Plast* 24(10):50–54. <https://doi.org/10.19491/j.issn.1001-9278.2010.10.010>
- Wang ZM, Hong H, Chung TC (2005) Synthesis of maleic anhydride grafted polypropylene with high molecular weight using borane/ O_2 radical initiator and commercial PP polymers. *Macromolecules* 38(22):8966–8970. <https://doi.org/10.1021/ma0516182>
- Bhattacharya A, Misra BN (2004) Grafting: a versatile means to modify polymers: techniques, factors and applications. *Prog Polym Sci* 29(8):767–814. <https://doi.org/10.1016/j.progpolymsci.2004.05.002>
- Rätzsch M, Arnold M, Borsig E, Bucka H, Reichelt N (2002) Radical reactions on polypropylene in the solid state. *Prog Polym Sci* 27(7):1195–1282. [https://doi.org/10.1016/S0079-6700\(02\)00006-0](https://doi.org/10.1016/S0079-6700(02)00006-0)
- Sathe SN, Srinivasa Rao GS, Devi S (1994) Grafting of maleic anhydride onto polypropylene: synthesis and characterization. *J Appl Polym Sci* 53(2):239–245. <https://doi.org/10.1002/app.1994.070530212>
- Patel AC, Brahmabhatt RB, Jain RC, Devi S (1998) Grafting of 2-HEMA on IPP and in situ chlorinated PP through solution polymerization. *J Appl Polym Sci* 69(11):2107–2113. [https://doi.org/10.1002/\(SICI\)1097-4628\(19980912\)69:11<2107:AID-APP2>3.0.CO;2-K](https://doi.org/10.1002/(SICI)1097-4628(19980912)69:11<2107:AID-APP2>3.0.CO;2-K)
- Sathe SN, Srinivasa Rao GS, Devi S (1993) Synthesis and characterization of PP-g-butyl acrylate copolymers. *Polym Int* 32(3):233–239. <https://doi.org/10.1002/pi.4990320304>
- Berzin F, Flat J-J, Vergnes B (2013) Grafting of maleic anhydride on polypropylene by reactive extrusion: effect of maleic anhydride and peroxide concentrations on reaction yield and products characteristics. *J Polym Eng* 33(8):673–682. <https://doi.org/10.1515/polyeng-2013-0130>
- Wang S-S, Zhao Z-Q, Wang N, Zhao J-R, Feng Y (2011) Structure and mechanism of functional isotactic polypropylene via in situ chlorination graft copolymerization. *Polym Int* 60(7):1068–1077. <https://doi.org/10.1002/pi.3044>
- Li Z, Ma Y, Yang W (2013) A facile, green, versatile protocol to prepare polypropylene-g-poly(methyl methacrylate) copolymer by water-solid phase suspension grafting polymerization using the surface of reactor granule technology polypropylene granules

- as reaction loci. *J Appl Polym Sci* 129(6):3170–3177. <https://doi.org/10.1002/app.39037>
16. Guo M, Zhang C, Xu J, Luo Z, Wei W (2016) An efficient, simple and facile strategy to synthesize polypropylene-*g*-(acrylic acid-*co*-acrylamide) nonwovens by suspension grafting polymerization and melt-blown technique. *Fibers Polym* 17(8):1123–1130. <https://doi.org/10.1007/s12221-016-6414-y>
 17. Zhou Q, Li M, Yao X, Lian Z, Zhang C, Wei W, Huang J (2014) Preparation of polypropylene chelating fibers by quenching pretreatment and suspension grafting and their Pb²⁺, adsorption ability. *Fiber Polym* 15(11):2238–2246. <https://doi.org/10.1007/s12221-014-2238-9>
 18. Kučera F, Petruš J, Bálková R, Jančář J (2020) Solid-state grafting of maleic anhydride onto polypropylene: the influence of morphology of polypropylene on heterogeneous reaction. *Polym Eng Sci* 60(5):1076–1082. <https://doi.org/10.1002/pen.25363>
 19. Chen F, Xie L (2020) Enhanced fouling-resistance performance of polypropylene hollow fiber membrane fabricated by ultrasonic-assisted graft polymerization of acrylic acid. *Appl Surf Sci* 502:144098. <https://doi.org/10.1016/j.apsusc.2019.144098>
 20. Jian W, Wang D, Wei D, Enguang Z, Qun D (2009) Supercritical carbon dioxide-assisted solid-phase free radical grafting of butyl acrylate onto PP. *e-Polymers* 9(1):1156–1170. <https://doi.org/10.1515/epoly.2009.9.1.1156>
 21. Tong G-S, Liu T, Hu G-H, Hoppe S, Zhao L, Yuan W-K (2007) Modelling of the kinetics of the supercritical CO₂ assisted grafting of maleic anhydride onto isotactic polypropylene in the solid state. *Chem Eng Sci* 62(18–20):5290–5294. <https://doi.org/10.1016/j.ces.2006.12.037>
 22. Kunita MH, Rinaldi AW, Girotto EM, Radovanovic E, Muniz EC, Rubira AF (2005) Grafting of glycidyl methacrylate onto polypropylene using supercritical carbon dioxide. *Eur Polym J* 41(9):2176–2182. <https://doi.org/10.1016/j.eurpolymj.2005.04.004>
 23. Wang W, Zhou S, Xin Z, Shi Y, Zhao S (2016) Polydimethylsiloxane assisted supercritical CO₂ foaming behavior of high melt strength polypropylene grafted with styrene. *Front Chem Sci Eng* 10(3):1–9. <https://doi.org/10.1007/s11705-016-1577-z>
 24. Yuan W, Wang F, Gao C, Liu P, Ding Y, Zhang S, Yang M (2020) Enhanced foamability of isotactic polypropylene/polypropylene-grafted-nanosilica nanocomposites in supercritical carbon dioxide. *Polym Eng Sci* 60(6):1353–1364. <https://doi.org/10.1002/pen.25386>
 25. Sun D, Wang B, He J, Zhang R, Liu Z, Han B, Huang Y (2004) Grafting of polypropylene with *N*-cyclohexylmaleimide and styrene simultaneously using supercritical CO₂. *Polymer* 45(11):3805–3810. <https://doi.org/10.1016/j.polymer.2004.03.063>
 26. Wang Y, Liu Z, Han B, Dong Z, Wang J, Sun D, Huang Y, Chen G (2004) pH Sensitive polypropylene porous membrane prepared by grafting acrylic acid in supercritical carbon dioxide. *Polymer* 45(3):855–860. <https://doi.org/10.1016/j.polymer.11.042>
 27. Spadaro G, De Gregorio R, Galia A, Valenza A, Filardo G (2000) Gamma radiation induced maleation of polypropylene using supercritical CO₂: preliminary results. *Polymer* 41(9):3491–3494. [https://doi.org/10.1016/S0032-3861\(99\)00588-1](https://doi.org/10.1016/S0032-3861(99)00588-1)
 28. Wang J, Li J, Li H, Zhou H (2020) Thermoplastic polyurethane (TPU) modifier to develop bimodal cell structure in polypropylene/TPU microcellular foam in presence of supercritical CO₂. *J Vinyl Addit Technol*. <https://doi.org/10.1002/vnl.21790>
 29. Wang D, Wang J (2017) Grafting dual polar monomers onto hydroperoxidized polypropylene with the assistant of supercritical carbon dioxide. *Appl Petrochem Res* 7(2–4):169–179. <https://doi.org/10.1007/s13203-017-0190-5>
 30. Zhu B, Dong W, Wang J, Song J, Dong Q (2012) Modification of polypropylene via the free-radical grafting ternary monomer in water suspension systems. *J Appl Polym Sci* 12(6):1844–1851. <https://doi.org/10.1002/app.36653>
 31. Wang J, Wang D, Du W, Zou E, Dong Q (2009) Synthesis of functional polypropylene via solid-phase grafting soft vinyl monomer and its mechanism. *J Appl Polym Sci* 113(3):1803–1810. <https://doi.org/10.1002/app.30179>
 32. Luo Z, Chen H, Xu J, Guo M, Lian Z, Wei W, Zhang B (2018) Surface grafting of styrene on polypropylene by argon plasma and its adsorption and regeneration of BTX. *J Appl Polym Sci* 135(17):46171. <https://doi.org/10.1002/app.46171>
 33. Nenglin C (2015) *Solvents handbook*. Chemical Industry Press, Beijing
 34. Wypych G (2019) *Handbook of solvents*. ChemTec Publishing, Toronto, pp 305–356
 35. Sato S, Gondo D, Wada T, Kanehashi S, Nagai K (2013) Effects of various liquid organic solvents on solvent-induced crystallization of amorphous poly(lactic acid) film. *J Appl Polym Sci* 129(3):1607–1617. <https://doi.org/10.1002/app.38833>
 36. Blackadder DA, Le Poidevin GJ (1976) Dissolution of polypropylene in organic solvents: 2. The steady state dissolution process. *Polymer* 17(9):768–776. [https://doi.org/10.1016/0032-3861\(76\)90031-8](https://doi.org/10.1016/0032-3861(76)90031-8)
 37. Blackadder DA, Le Poidevin GJ (1976) Dissolution of polypropylene in organic solvents: 1. Partial dissolution. *Polymer* 17(5):387–394. [https://doi.org/10.1016/0032-3861\(76\)90233-0](https://doi.org/10.1016/0032-3861(76)90233-0)
 38. Galia A, De Gregorio R, Spadaro G, Scialdone O, Filardo G (2004) Grafting of maleic anhydride onto isotactic polypropylene in the presence of supercritical carbon dioxide as a solvent and swelling fluid. *Macromolecules* 37(12):4580–4589. <https://doi.org/10.1021/ma049880i>
 39. Hou Z, Xu Q, Peng Q, Li J, Fan H, Zheng S (2006) Different factors in the supercritical CO₂-assisted grafting of poly(acrylic acid) to polypropylene. *J Appl Polym Sci* 100(6):4280–4285. <https://doi.org/10.1002/app.23857>
 40. Miller-Chou BA, Koenig JL (2003) A review of polymer dissolution. *Prog Polym Sci* 28(12):1223–1270. [https://doi.org/10.1016/S0079-6700\(03\)00045-5](https://doi.org/10.1016/S0079-6700(03)00045-5)
 41. Dong Z, Liu Z, Han B, Pei X, Liu L, Yang G (2004) Modification of isotactic polypropylene films by grafting methyl acrylate using supercritical CO₂ as a swelling agent. *J Supercrit Fluid* 31(1):67–74. <https://doi.org/10.1016/j.supflu.2003.09.020>
 42. Wang D, Xu W, Sun G, Chiou B (2011) Radical graft polymerization of an allyl monomer onto hydrophilic polymers and their antibacterial nanofibrous membranes. *ACS Appl Mater Interfaces* 3:2838–2844. <https://doi.org/10.1021/am200286a>
 43. Pan Z (2003) *Polymer chemistry*. Chemical Industry Press, Beijing, pp 27–29
 44. Nelson ED, Thompson GM, Yao Y, Flanagan HM, Harmon PA (2009) Solvent effects on the AIBN forced degradation of cumene: implications for forced degradation practices. *J Pharm SCI-US* 98(3):959–969. <https://doi.org/10.1002/jps.21489>
 45. Zhang M, Colby RH, Milner ST, Chung TCM (2013) Synthesis and characterization of maleic anhydride grafted polypropylene with a well-defined molecular structure. *Macromolecules* 46(11):4313–4323. <https://doi.org/10.1021/ma400663z>
 46. Zhao C, Okada H, Sugimoto R (2018) Surface modification of polypropylene with poly(methyl methacrylate) initiated by a diethylzinc and 1,10-phenanthroline complex. *React Funct Polym* 132:127–132. <https://doi.org/10.1016/j.reactfunctpolym.2018.09.012>
 47. Abudonia KS, Saad GR, Naguib HF, Eweis M, Zahran D, Elsabee MZ (2018) Surface modification of polypropylene film by grafting with vinyl monomers for the attachment of chitosan. *J Polym Res* 25:125. <https://doi.org/10.1007/s10965-018-1517-3>
 48. Wang S, Zhang X, Jiang C, Jiang H, Tang Y, Li J, Ren M, Qiao J (2019) Polymer solid-phase grafting at temperature higher than

the polymer melting point through selective heating. *Macromolecules* 52(9):3222–3230. <https://doi.org/10.1021/acs.macromol.8b02737>

Publisher's Note Springer Nature remains neutral with regard to jurisdictional claims in published maps and institutional affiliations.